



RESEARCH ARTICLE

ANDERSON-TYPE POMs, SYNTHESIS AND ELECTROCHEMICAL AND PHOTO-CHROMISM PROPERTIES STUDIES

Papa Aly Gueye, Lamine Yaffa, Ababacar Diouf, Antoine Blaise Kama, Daouda Ndoye, Bocar Traoré, Cheikh A.K. Diop, Mamadou Sidibé and Romain Gautier

Manuscript Info

Manuscript History

Received: 05 October 2024

Final Accepted: 07 November 2024

Published: December 2024

Key words:-

Anderson-Type, Polyoxometalate, Electrochemical, Photochromic

Abstract

Two compounds of polyoxometalate, $(\text{NH}_4)_5[\text{IMo}_6\text{O}_{24}] \cdot 3\text{NH}_3 \cdot 5\text{H}_2\text{O}$ (1) and $(\text{NH}_4)_6[\text{TeMo}_6\text{O}_{24}] \cdot \text{NH}_3 \cdot 5\text{H}_2\text{O}$ (2), have been synthesized and characterized by elemental analysis; IR and UV-visible spectroscopy; TG analysis; and single-crystal X-ray diffraction. The crystal data for these compounds are the following: **1**, orthorhombic, Pccn, $a=14.2765(4)$ Å, $b=14.9384(3)$ Å, $c=14.6053(3)$ Å, $\alpha=90^\circ$, $\beta=90^\circ$, $\gamma=90^\circ$, $Z=10$; **2**, orthorhombic, Pccn, $a=14.2538(5)$ Å, $b=14.9475(5)$ Å, $c=14.6598(5)$ Å, $\alpha=90^\circ$, $\beta=90^\circ$, $\gamma=90^\circ$, $Z=10$. Compounds 1 and 2 exhibited 2D networks derived from Anderson A-type $[\text{XMo}_6\text{O}_{24}]^{5-}$ ($\text{X}=\text{I}$ (**1**) or Te (**2**)) anions; H_2O and $\text{NH}_Y^{(Y-3)+}$ ($Y=3$ or 4). The electrochemical and photochromic properties of these compounds were studied. And it reveals that compound (**2**) shows excellent redox and photochromic properties. Unlike compound (**1**) which has good redox properties but weak photochromic properties.

Copyright, IJAR, 2024., All rights reserved.

Introduction:-

Polyoxometalates (POMs) are a broad class of polynuclear molecular oxide anions generally formed by W, Mo or V in high oxidation states.¹ Due to their exceptional properties, polyoxometalates have a wide range of applications in which the most common are catalysis, materials chemistry, medicine, water chemistry and electrochemistry²⁻⁵. This diversity of applications drives many researchers to take an interest in the synthesis of these compounds, which has led to a vast expansion of polyoxometalates. Thus, the polyoxometalates are represented by families possessing well-defined structures, among which there is: Keggin^{6,7} $[\text{XM}_{12}\text{O}_{40}]^{n-}$, Anderson⁸ $[\text{H}_6\text{XM}_6\text{O}_{24}]^{n-}$, Lindqvist^{9,10} $[\text{MxM}'_6\text{xO}_{19}]^{(2+x)-}$ and Dawson¹¹ $[\text{X}_2\text{M}_{18}\text{O}_{62}]^{n-}$. In recent years, there has been particularly an increasing interest in the chemistry of Anderson-type POMs compounds.¹² These polyanions of general formula $[\text{Hy}(\text{XO}_6)\text{M}_6\text{O}_{18}]^{n-}$ ($y=0-6$, $n=2-8$, $\text{M}=\text{W}$; Mo atom, $\text{X}=\text{heteroatom}$) represent one of the basic structures of polyoxometalates^{13,14} and, thanks to their flexibilities, they can be modified by various means: (a) altering the central heteroatom; (b) incorporating inorganic and/or organic cations to build coordination or supramolecular architectures; and (c) covalent linkage with organic moieties to functional yield hybrids.¹⁵⁻¹⁸ Thus, the precious selection of the heteroatom and the organic group has become a challenge for the synthesis of new the Anderson-type hybrids. As a result, the choice of halogens and chalcogens such as iodine and tellurium attract considerable attention. This is not only because of their fantastic variety of architectures and topologies¹⁹⁻²² but also because of their many potential applications in catalytic chemistry, optics and magnetism. Thus, many strategic methods for synthesizing Anderson-type POMs hybrids have been developed and published in scientific journals.

Among these methods of synthesis, the most commonly used are: deforming the structure, forming an electronic gap in the compound, and replacing one metal with other metals.

As part of our ongoing efforts to synthesize polyoxometallate materials, we reported two compounds $(\text{NH}_4)_5[\text{IMo}_6\text{O}_{24}] \cdot 3\text{NH}_3 \cdot 5\text{H}_2\text{O}$ and $(\text{NH}_4)_6[\text{TeMo}_6\text{O}_{24}] \cdot \text{NH}_3 \cdot 5\text{H}_2\text{O}$. Among the latter are, for each compound, an Anderson-type polyoxoanion whose heteroatoms are iodine and tellurium, respectively. Thus, in this work we study the photochromic, electrochemical and thermal properties of these two compounds.

Experimentalsection

Chemical materials Ammonium heptamolybdate tetrahydrate $(\text{NH}_4)_6[\text{Mo}_7\text{O}_{24}] \cdot 4\text{H}_2\text{O}$ (98%), iodic acid (98%), and telluric acid (99%) were purchased from Sigma-Aldrich and used without further purification with distilled water. Chemical preparation

Synthesis of $(\text{NH}_4)_5[\text{IMo}_6\text{O}_{24}] \cdot 3\text{NH}_3 \cdot 5\text{H}_2\text{O}$ (1,764g) (1)

Direct functionalization method with one pot synthesis process was carried out by mixing, in 40mL of distilled water, 3.707g of ammonium heptamolybdate $(\text{NH}_4)_6[\text{Mo}_7\text{O}_{24}] \cdot 4\text{H}_2\text{O}$ and iodic acid (HIO_3) for functionalize, chlorhydric acid was used to acidify and adjust the pH solutions to 5.4.

Synthesis of $(\text{NH}_4)_6[\text{TeMo}_6\text{O}_{24}] \cdot \text{NH}_3 \cdot 5\text{H}_2\text{O}$ (3,24g) (2)

Direct functionalization method with one pot synthesis process was carried out by dissolving, in 30mL of distilled water 3.707g of ammonium heptamolybdate $(\text{NH}_4)_6[\text{Mo}_7\text{O}_{24}] \cdot 4\text{H}_2\text{O}$ and telluric acid (H_6TeO_6) for functionalize, chlorhydric acid was used to acidify and adjust the pH solutions to 7.4.

Booth the solutions were heated under reflux and agitation for two hours. Then, the colorless solutions were cooled to room temperature and filtered. After 2 weeks of slow evaporation at room temperature, colorless crystals suitable for single-crystal X-ray diffraction were isolated in about 45% and 83% yield (based on Mo) respectively (1) and (2).

X-raycrystallography

A single-crystal X-ray diffraction data, for booth compounds, were measured on a Rigaku Oxford Diffraction Supernova diffractometer at the $\text{MoK}\alpha$ radiation. Data collection reduction and multi-scan ABSPACK correction were performed with CrysAlisPro (Rigaku Oxford Diffraction). For both compounds, the crystal structures including the anisotropic displacement parameters were refined with SHELXL-2013²³. PLATON²⁴ was used to check additional symmetry elements and Crystallographic Information Files were compiled with Olex2.12. Crystallographic data are summarized in Table 1.

Spectroscopy

The UV-Visible absorption measurements of booth compound were recorded using a Thermo Scientific GENESYS 10S UV-Vis spectrophotometer at room temperature in acidic aqueous solution (H_2SO_4). For all compounds, 15 mg was solubilized in 10ml of sulfuric acid solution (2M).

A scan between 200 nm and 1100 nm was carried out for each compound. Sulfuric acid /distilled water was used as blank.

IR spectroscopy measurements were carried out for both compounds. IR measurements were performed using ATR(Attenuated Total Reflectance) method from 4000 to 400 cm^{-1} .²⁵

Thermogravimetric measurement and Differential Scanning Calorimetry

Thermogravimetric (TG) and Differential Scanning Calorimetry (DSC) measurements were carried out with a SetaramSensysEvo under Argon flow, from room temperature to 800 °C, with a heating rate of 5 °C/min.

Photochromic properties measurement

Photochromic properties of booth compounds were evaluated at room temperature with a UV-lamp (254 nm /365nm; 2X6W UVGL-58).

Electrochemical properties measurement

Electrochemical measurements were carried out using a DropSens-Stat-I 400 as a potentiostat/galvanostat instrument. They were performed using three electrodes cell consisting of a glassy carbon electrode (0.07cm² surface area) as the working electrode, a reference electrode (Ag/AgCl, 1M KCl saturated) and a platinum wire as the counter electrode.

Results and Discussion:-

Structures description

Single-crystal X-ray diffraction was performed on a single crystal of both compounds.

It reveals that both compounds crystallize in orthorhombic system with space group Pccn.

The asymmetric unit of (1) contains one iodomolybdate Anderson-type polyanion [IMo₆O₂₄]⁵⁻, five ammonium molecules (NH₄)⁺, three neutral ammoniac (NH₃) molecules and five water molecules (H₂O) (Figure. 1). For the compound (2), the asymmetric unit contains one telluromolybdate Anderson-type polyanion [TeMo₆O₂₄]⁶⁻, six ammonium molecules (NH₄)⁺, one ammoniac (NH₃), and five water molecules (H₂O) (Figure. 1). Both clusters of compounds (1) and (2) has an A-type Anderson structure [IMo₆O₁₈]⁵⁻ and [TeMo₆O₂₄]⁶⁻ respectively, (general formula: [(XO₆)M₆O₁₈]ⁿ⁻ (n = 2-8, M = addenda atom, X = heteroatom).

From the structural point of view, the topological structure of polyanions consists of six {MoO₆} octahedra forming an hexagon around the central {XO₆} with X = I, Te respectively (1) et (2)) octahedron (Figure 2). In structural architecture of the polyanions, the oxygen atoms are divided into three groups leading to four sets Mo—O bonds for each anion (Figure 2) : (a) the Mo—O_t bonds (O_t = terminal oxide) are the shortest and are in the order of with bond lengths range = 1.707(4)–1.713(4) Å; for compound (1) and 1.708(3)–1.716(4) Å for compound (2); (b) Mo—Ob1 medium lengths (Ob1 = oxygen atoms bridging two molybdenum atoms) and are in the order of 1.923(4)–1.941(4) Å for compound (1), and 1.921(3)–1.943(3) Å for compound (2); (c) Mo—Ob2 the longest bond of the compound (Ob2 = oxygen atoms shared by two molybdenum atoms and one tellurium or iodine atom) with bond lengths range of 2.277(3)–2.296(3) Å for compound (1) and 2.272(3)–2.3295(3) Å for compound (2). The I—O distances range from 1.923(4)–1.933(4) Å for compound (1) and Te—O from 1.927(3)–1.935(3) Å for compound (2).

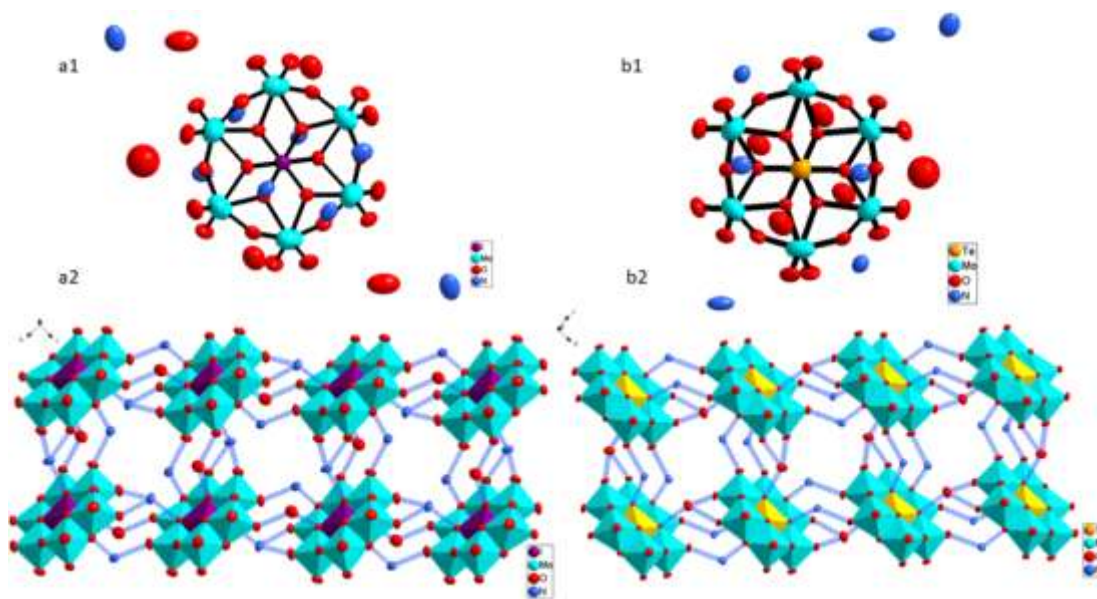


Figure 1:- Three-dimensional and ellipsoidal representation of compounds a1 and a2 for compound 1, as well as b1 and b2 for compound 2.

From the structural point of view, the topological structure of polyanions consists of six {MoO₆} octahedra arrange hexagonally around the central {XO₆} (X = I, Te respectively (1) et (2)) octahedron (Figure 2).In structural architecture of the polyanions, according to the way the oxygen atoms are coordinated, the oxygen atoms are divided

into three groups leading to four sets Mo—O bonds for each anion (Figure 2) : (a) the Mo—O_t bonds (O_t = terminal oxide) are the shortest and are in the order of with bond lengths range = 1.707(4)–1.713(4) Å; for compound (1) and 1.708(3)–1.716(4) Å and for compound (2); (b) Mo—Ob1 medium lengths (Ob1 = oxygen atoms bridging two molybdenum atoms) and are in the order of 1.923(4)–1.941(4) Å for compound (1), and 1.921(3)–1.943(3) Å for compound (2); (c) Mo—Ob2 the longest bond of the compound (Ob2 = oxygen atoms shared by two molybdenum atoms and one tellurium or iodine atom) with bond order of 1.923(4)–1.941(4) Å for compound (1), and 1.921(3)–1.943(3) Å for compound (2); (c) Mo—Ob2 the longest bond of the compound (Ob2 = oxygen atoms shared by two molybdenum atoms and one tellurium or iodine atom) with bond lengths range of 2.277(3)–2.296(3) Å for compound (1) and 2.272(3)–2.3295(3) Å for compound (2). The I—O distances range from 1.923(4)–1.933(4) Å for compound (1) and Te—O from 1.927(3)–1.935(3) Å for compound (2).

Table 1:- Crystallographic data for compounds 1 and 2.

Compounds	1	2
Empirical formula	H ₃₉ N ₈ IMo ₆ O ₂₉	H ₃₇ N ₇ TeMo ₆ O ₂₉
Formula weight	1317.95	1302.63
Crystal system	Orthorhombic	Orthorhombic
Space group	Pccn	Pccn
a(Å)	14.2765(4)	14.2538(5)
b(Å)	14.9384(3)	14.9475(5)
c(Å)	14.6053(3)	14.6598(5)
α(°)	90	90
β(°)	90	90
γ(°)	90	90
V (Å ³)	3114.84(12)	3123.4(2)
Z	10	5
D _x (Mg.m ⁻³)	2.475	2.657
F(000)	2158	2309
λ(Å)	0.71073	0.71073
T(K)	297	297
θ(°) range	3.4 ≤ θ ≤ 26.4	3.4 ≤ θ ≤ 26.2
Absorption coefficient (mm ⁻¹)	3.60	3.36
hkl range	-17 ≤ h ≤ 16 ; -18 ≤ k ≤ 18 ; -18 ≤ l ≤ 17	-17 ≤ h ≤ 16 ; -18 ≤ k ≤ 18 ; -18 ≤ l ≤ 17
Final R indices	R = 0.084 ; wR(F ²) = 0.110	R = 0.063 ; wR(F ²) = 0.092
Reflections collected	43692	42007
Independent reflections	2941	2948
Largest diff. peak/hole (e Å ⁻³)	-1.16/0.95	-0.83/1.04

The inter metallic bonds Mo—Mo and Mo—I are in the range of 3.263(1)–3.294(1)Å and 3.273(1)–3.294(1)Å for compound (1) and Mo—Mo and Mo—Te in the range of 3.261(1)–3.293(1) Å et 3.277(1)–3.295(1) Å for compound (2).

In the polyanion of both compounds, the octahedral unit, IO₆ or TeO₆ are surrounded by six MoO₆ groups, forming a hexagon respectively around I or Te, giving overall approximate D_{2h} symmetry to the anion. The central heteroatoms I^{VII+} or Te^{V+} are octahedral link by six Ob2 oxygen atom type (O005 ; O006 ; O007)

The bond angles of O—I—O_{cis} range from 85.55°(14) to 94.45°((14) and O—I—O_{trans} is 180° and the link O—Te—O_{cis} angles range from 85.69(15) to 94.31 (15) and O—I—O_{trans} is 180°.

In both compounds, as shown in Figure 1, it is striking that the structures exhibits extensive hydrogen-bonding interactions among water molecules, ammoniac molecules, ammonium molecules and polyoxoanions. The typical hydrogen bonds distances are as follows : for compound (1) : O008...N00K= 2.715(7)Å, O00G...N00K= 2.856(7)Å, O005...N00H=2.836(7)Å, O00F...N00H= 2.896(7)Å, O00E...N00H=2.941(7)Å, O00J...O00B= 2.857(7)Å, O00J...O007= 2.844(7)Å and for compound (2) : O009...N00J= 2.710(6)Å;N00J...O00F= 2.885(7)Å; O00G...O00I= 2.901(5)Å; O00I...O005=2.844(5)Å; O00D...N00K= 2.859(6)Å; N00K...O006= 2.838(6)Å; O00E...O00I= 2.949(6)Å for compound (2).

The bond valence sum calculations²⁶ indicate that I site is in the +7 oxidation state, Te site is in the +6 oxidation state and all Mo sites are in the +6 oxidation state respectively in compound 1 and 2. Which means that for the stabilization of the clusters, the polyanion of 1 is surrounded with five organic ammonium molecules to counterbalance the charge and six organic ammonium molecules around the polyanion of 2.

Moreover, for both compounds, the two asymmetric polyanion monomers are further linked with each other to form a very stable dimeric, trimeric, and tetrameric structure through hydrogen bonds between the bridging oxo and terminal oxo ligands of the polyanions, which is similar to the formation of those kinds of structures based Anderson-type POMs.²⁷ This hydrogen bonds network lead to the formation of an infinite 1D chain in zig-zag then each chains are connected with hydrogen bonds to neighbors parallel chains to give a 3D supramolecular network (Figure 1).

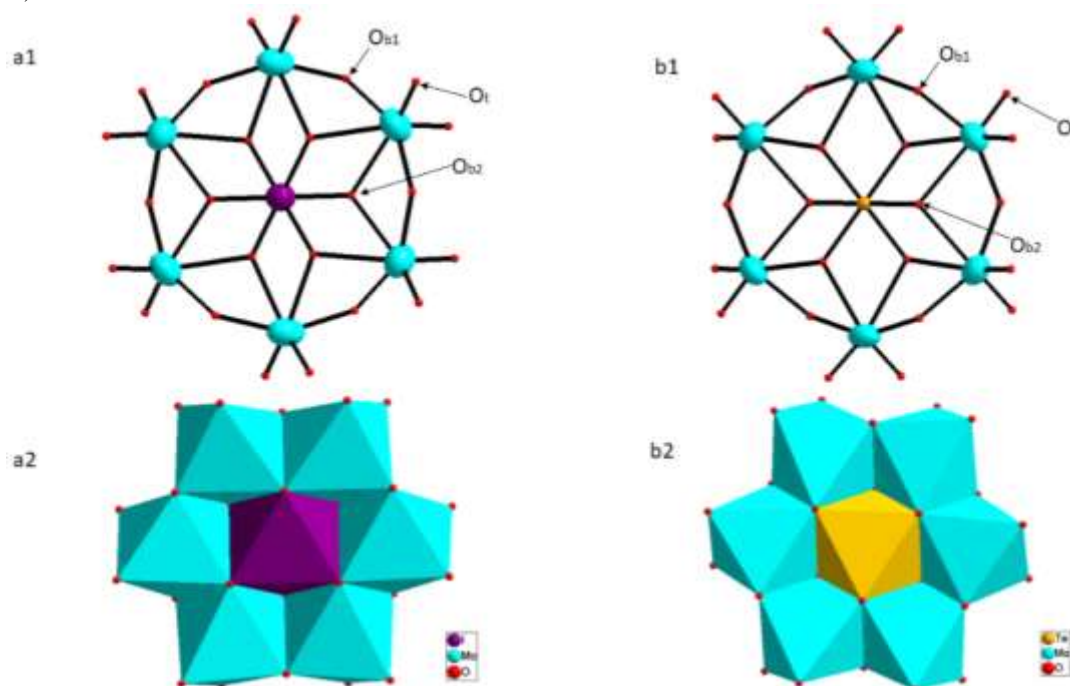


Figure 2:- Representation of the polyanions of the compounds; a1 and b1: ORTEP drawing, a2 and b2 : polyhedral.

UV-vis and IR spectroscopy

The IR spectrum of both compounds is shown in Figure 3. The characteristic bands observed at 937, 876, 680 cm^{-1} for 1; 921, 868, 665 cm^{-1} for 2 are attributed to $\nu(\text{Mo}-\text{O}_t)$ and $\nu(\text{Mo}-\text{O}-\text{Mo})$, respectively^{14,27,28} confirming the Anderson-type polyanion formation. The bands between 2800 and 3400 cm^{-1} of average intensity are probably the result of the $\nu(\text{N}-\text{H})$ vibrations of the ammonium and ammoniac groups. The broad bands around 3600 cm^{-1} can be ascribed to the water molecules.

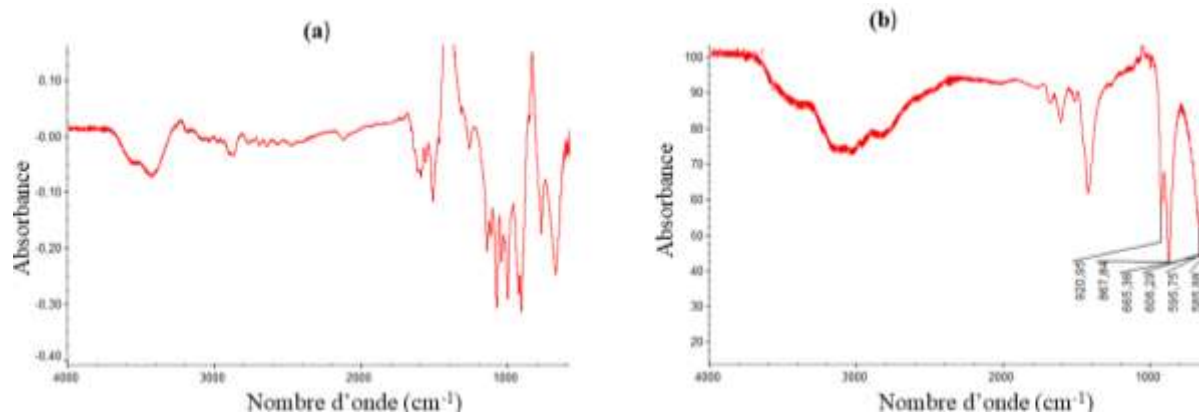


Figure 3:- IR spectra of compounds.

The UV–Visible absorption of both compounds was analyzed in the 200–700 nm range in acidic solution. In the UV-vis region, only one single strong absorption band is observed for both compounds. The UV spectra reveal precisely absorption peak at λ_{max} equal 298nm and 296nm for compounds (1) and (2), respectively (Figure 4). This absorption band is attributed to Ligand-Metal Charge Transfer (LMCT) transition of the $\text{O} \rightarrow \text{Mo}^{29-31}$. Indeed, during irradiation, electrons are promoted from low-energy electronic states, mainly composed of 2p oxygen orbitals, to the high-energy electron states, mainly made up of 4d metal orbitals of molybdenum. Then, both compounds absorb in the ultraviolet region.

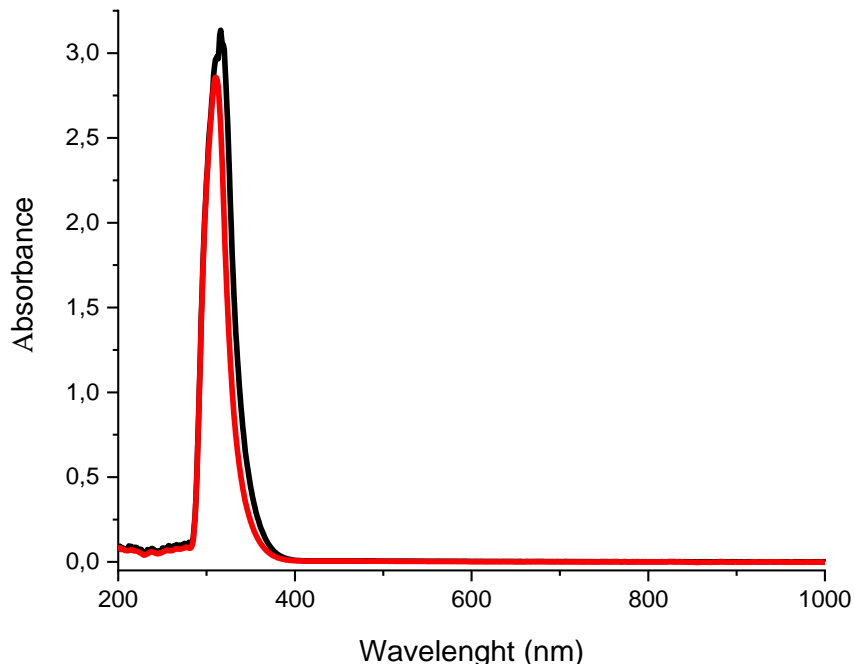


Figure 4:- UV–visible spectra of the compounds: compound 1(black); compound 2 (red).

TG/DSC analysis

In order to examine the thermal stability, TG and DSC analyses of both compounds were carried out from room temperature to 800 °C (Figure 5).

The TG data for compound (1) shows three weight losses. The first loss of 7.24% between 30 and 150 °C would correspond to the loss of five water molecules of the single crystal when dried under vacuum (calculated loss: 6.87%). In this range, this weight loss can be seen with an exothermic peak of the DSC curve. The second weight loss of 9.2 % between 150 and 230 °C corresponds to the decomposition of eight NH_3 (calculated loss: 10.3%). In this range, the DSC curve shows another endothermic peak. The last loss starting from 230 °C corresponds to the degradation of the cluster.

The TG curve for compound (2) shows many weight losses. The first weight loss of 7% observed between 25 and 125°C (calculated 6.91%) corresponds to the degradation of the five crystallization water molecules. In this range, the DSC curve shows an exothermic peak. The second weight loss of 10% (calculated 9.62%) attributed to amino groups molecules; this weight loss is observed between 125 and 325°. Starting at 340°C, we notice that the diagram is stable, which constitutes a phase transition whose polyanion transforms into oxide before degrading around 700°C.

The thermogravimetric curve shows total weight loss of 75% for compound (1) and 40% for compound (2).^{28,32}

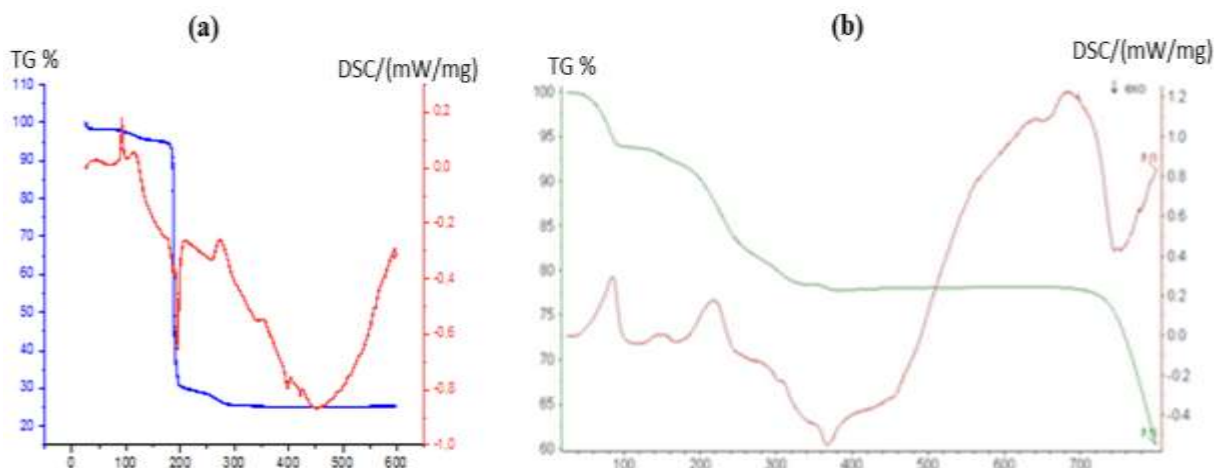


Figure 5:- TG and DSC curves of the compounds (a) for compound 1 and (b) for compound 2.

Photochromic proprieties

Photochromic is defined as the ability of a molecule or material to change color reversibly under the effect of electromagnetic irradiation in the ultraviolet, visible or infra-red ranges.

Thus, the photochromic compartment of both compounds were demonstrated under a UV lamp with the excitation at a wavelength of 254 nm (4.89 eV) and 365 nm (3.4 eV). All the crystals materials show a colorless coloration in their ground state. Under UV excitation at 365 nm (3.4 eV), only the compound (2) has photochromic response after five minutes of irradiation. There is no change in color at 254 nm (4.89 eV).

However, the compound (1) has photochromic response after one hours of irradiation under UV excitation at 254 nm (4.89 eV).

After five-minute UV excitation under the lamp, the color of compound (2) changed from colorless to brown and the material show strong photochromic response with high coloration, as contrast the photoinduced color become increasingly intense with time (Figure 6b). The photo-induced color did not change after one hour of irradiation. However, the return to the original color requires a long time at room temperature (i.e. 1 hours) or 3min at 50°C.

Based on the literature the coloration is then due to the photoreduction of central metals. This reduction is generated by, during the absorption of a photon, the homolytic breaking of the N-H bond leads to the transfer of the hydrogen atom to the terminal oxygen ligand of the polyanion^{34,35}. The oxygen atoms transfer their electrons to the central metal the Mo^{VI} whose are reduced to Mo^V. The Mo^V cations with a d¹ electronic configuration may then be involved in d-d transitions or intervalence Mo^V+ Mo^{VI} → Mo^{VI}+ Mo^V charge transfer inducing new colors³³⁻³⁶.

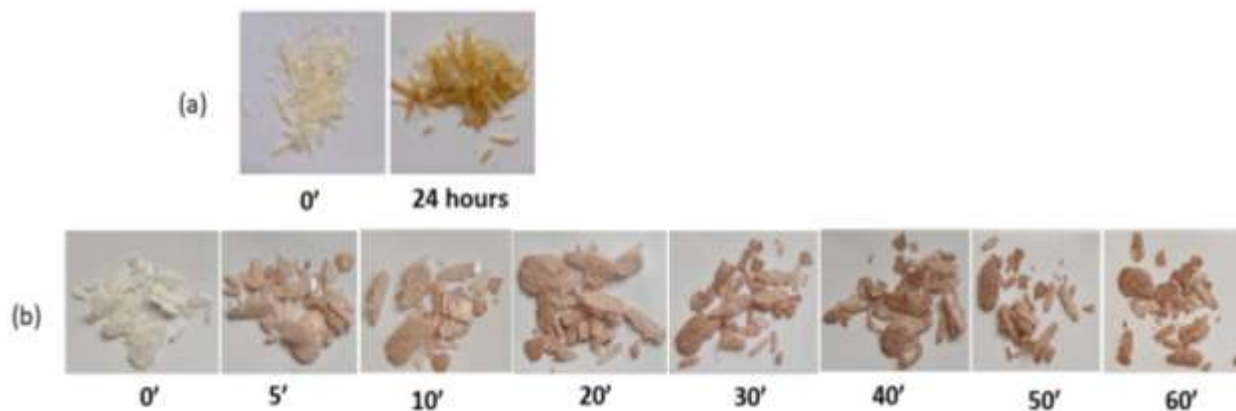


Figure 6:- Color of Compounds after UV irradiation: (a): compound (1), (b): compound (2).

Electrochemistry

In the potential range from -0.8 V to +1.5 V, the cyclic voltammogram of compounds 1 and 2 at respective scan rate of **15 mV/s** and 5 mV/s shows two reduction peaks. For compound (1), the two redox peaks are located at the mean peak potentials $\frac{1}{2}E = \frac{1}{2}(E_{pa} + E_{pc})$ at **-67,208 mV (I-I')** and **-52,8955 mV (II-II')** respectively (Figure 7). For compound (2), the two redox peaks are observed at the mean peaks potentials equal to **1,8125 mV (I-I')** and **-29,375 mV (II-II')** respectively (Figure 8).

The two reduction peaks correspond to two consecutive one-electron processes based on molybdenum centers.³⁷⁻³⁹ The cyclic voltammetry (CV) curves of the glassy carbon electrodes of the compound, obtained at scan rates ranging from 5 to 45 mV/s are represented (Figure 7a3, 8b3). The peak currents densities and the peak potential difference values of these oxidation/reduction processes on the electrode, increase with the scan rate, indicating these processes are reversible.

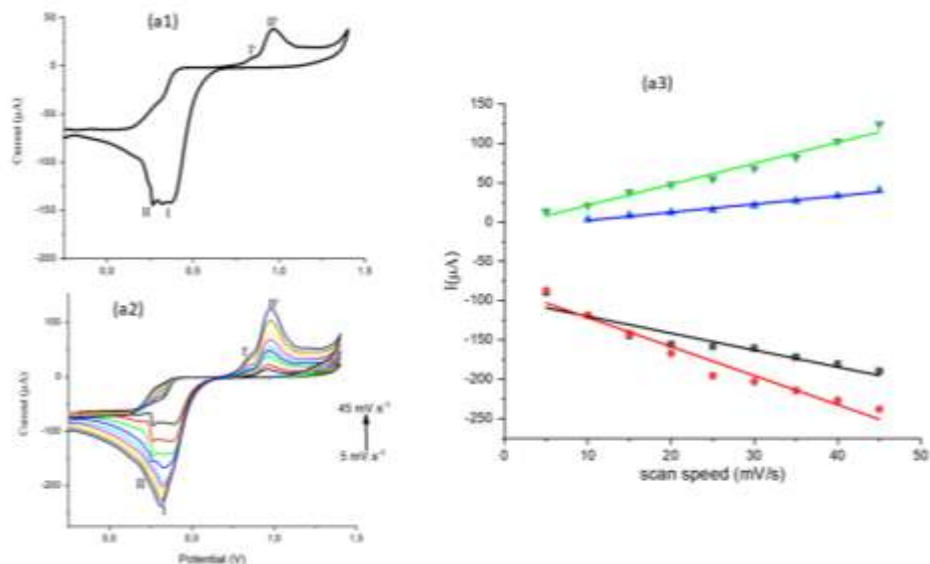


Figure 7:- Electrochemical measurements of compound (1): (a₁: Cyclic voltammograms at scan rate = X mV/s, a₂: Cyclic voltammograms with different scan rates; a₃ Calibration curve for peak currents with respect to the root of the scanning speed.)

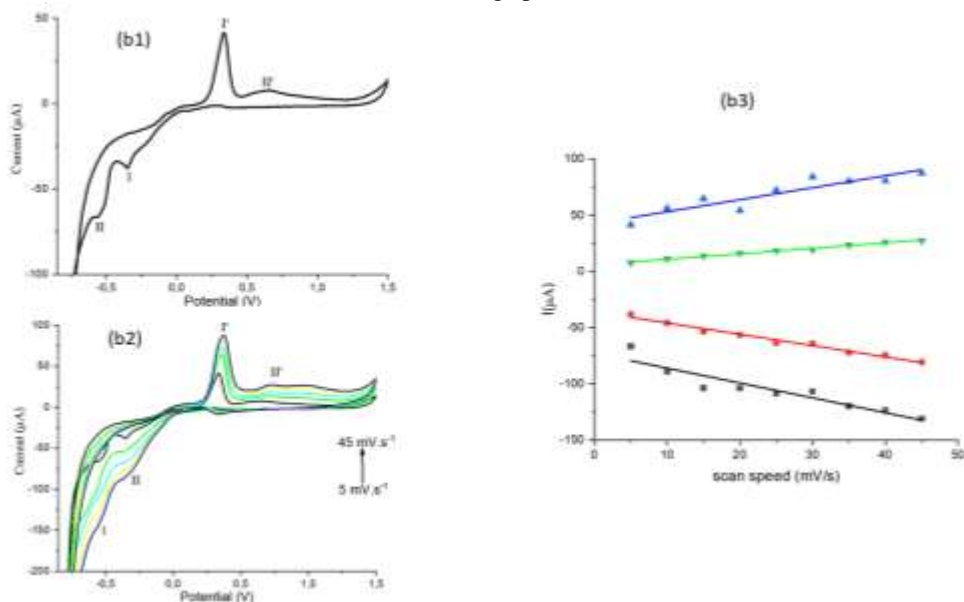


Figure 8:- Electrochemical measurements of compound (1) : (a₁: Cyclic voltammograms at scan rate = X mV/s, a₂: Cyclic voltammograms with different scan rates; a₃ Calibration curve for peak currents with respect to the root of the scanning speed).

Conclusion:-

In this work, we successfully synthesized two Anderson-type POM through a reflux method which provides novel examples of the utilities of synthesized Anderson clusters as interated with ammonium and water molecules for constructing extended solid-state materials.

The structure of both compounds possesses a 3D supramolecular structure composed of ammonium, water and polyanion layers pillared chains. The present work may supply a potential method for forming other related pillared structures via alterations to POM building blocks or central heteroatom.

The electrochemical properties of the title compounds were investigated and show for both compounds two reversible consecutive one-electron redox and the scan rate indicates a process controlled by surface. Both compounds are built of Anderson type polyanion with same organic counterions like ammonium and water molecules. But the photochromic properties study of both compounds under a UV lamp with the excitation show that the compound (2) is photochrom five minutes after irradiation at a wavelength of 365nm and the compound (1) at 254nm after 1 hours of UV irradiation.

These results show that for Anderson types-POMs not only the large numbers of hydrogen bonds interactions are responsible for photochromic properties but the the nature of central heteroatom play a key role for the photo-reduction properties. Therefore, the choice of basic materials building units can influence profoundly the structure of synthesized products and to direct their formation with particular structural and physical properties.

Acknowledgments:-

The authors gratefully acknowledge the Cheikh Anta Diop University – Dakar (Senegal), Institute of des Matériaux de Nantes Jean Rouxel (France).

References:-

- (1) Long, D.-L.; Burkholder, E.; Cronin, L. Polyoxometalate Clusters, Nanostructures and Materials: From Self Assembly to Designer Materials and Devices. *Chem. Soc. Rev.* 2007, 36 (1), 105–121. <https://doi.org/10.1039/B502666K>.
- (2) Katsoulis, D. E. A Survey of Applications of Polyoxometalates. *Chem. Rev.* 1998, 98 (1), 359–388.
- (3) Piera, J.; Baeckvall, J.-E. Catalytic Oxidation of Organic Substrates by Molecular Oxygen and Hydrogen Peroxide by Multistep Electron Transfer—a Biomimetic Approach. *Angew. Chem. Int. Ed.* 2008, 47 (19), 3506–3523.
- (4) Hill, C. L. Progress and Challenges in Polyoxometalate-Based Catalysis and Catalytic Materials Chemistry. *J. Mol. Catal. Chem.* 2007, 262 (1–2), 2–6.
- (5) Mizuno, N.; Yamaguchi, K. Polyoxometalate Catalysts: Toward the Development of Green H₂O₂-Based Epoxidation Systems. *Chem. Rec.* 2006, 6 (1), 12–22.
- (6) Pauling, L. The Molecular Structure of the Tungstosilicates and Related Compounds. *J. Am. Chem. Soc.* 1929, 51 (10), 2868–2880.
- (7) Keggin, J. F. Structure of the Molecule of 12-Phosphotungstic Acid. *Nature* 1933, 131 (3321), 908–909.
- (8) Anderson, J. S. Constitution of the Poly-Acids. *Nature* 1937, 140 (3550), 850–850.
- (9) Bustos, C.; Hasenknopf, B.; Thouvenot, R.; Vaissermann, J.; Proust, A.; Gouzerh, P. Lindqvist-Type (Aryldiazenido) Polyoxomolybdates- Synthesis, and Structural and Spectroscopic Characterization of Compounds of the Type (nBu₄N)₃ [Mo₆O₁₈(N₂Ar)]. *Eur. J. Inorg. Chem.* 2003, 2003 (15), 2757–2766.
- (10) Proust, A.; Thouvenot, R.; Roh, S.-G.; Yoo, J.-K.; Gouzerh, P. Lindqvist-Type Oxo-Nitrosyl Complexes. Syntheses, Vibrational, Multinuclear Magnetic Resonance (14N, 17O, 95Mo, and 183W), and Electrochemical Studies of [M₅O₁₈{M'(NO)}₃]- Anions (M, M' = Mo, W). *Inorg. Chem.* 1995, 34 (16), 4106–4112. <https://doi.org/10.1021/ic00120a014>.
- (11) Souchay, P. Tungstic Heteropolyacids. VIII. Phosphotungstates. *Ann Chim* 1947, 2, 203–222.
- (12) Nikulshin, P.; Mozhaev, A.; Lancelot, C.; Blanchard, P.; Payen, E.; Lamonier, C. Hydroprocessing Catalysts Based on Transition Metal Sulfides Prepared from Anderson and Dimeric Co₂Mo₁₀-Heteropolyanions. A Review. *Comptes Rendus Chim.* 2016, 19 (10), 1276–1285. <https://doi.org/10.1016/j.crci.2015.10.006>.
- (13) Ying, J.; Chen, Y.-G.; Wang, X.-Y. A Series of 0D to 3D Anderson-Type Polyoxometalate-Based Compounds Obtained under Ambient and Hydrothermal Conditions. *CrystEngComm* 2019, 21 (7), 1168–1179.

- (14) Li, J.-H.; Wang, X.-L.; Song, G.; Lin, H.-Y.; Wang, X.; Liu, G.-C. Various Anderson-Type Polyoxometalate-Based Metal–Organic Complexes Induced by Diverse Solvents: Assembly, Structures and Selective Adsorption for Organic Dyes. *Dalton Trans.* 2020, 49 (4), 1265–1275.
- (15) Caudillo-Flores, U.; Ansari, F.; Bachiller-Baeza, B.; Colón, G.; Fernández-García, M.; Kubacka, A. (NH₄)₄ [NiMo₆O₂₄H₆]. 5H₂O/g-C₃N₄ Materials for Selective Photo-Oxidation of CO and CC Bonds. *Appl. Catal. B Environ.* 2020, 278, 119299.
- (16) Sun, L.; Su, T.; Xu, J.; Hao, D.; Liao, W.; Zhao, Y.; Ren, W.; Deng, C.; Lü, H. Aerobic Oxidative Desulfurization Coupling of Co Polyanion Catalysts and P-TsOH-Based Deep Eutectic Solvents through a Biomimetic Approach. *Green Chem.* 2019, 21 (10), 2629–2634.
- (17) Chi, M.; Zhu, Z.; Sun, L.; Su, T.; Liao, W.; Deng, C.; Zhao, Y.; Ren, W.; Lü, H. Construction of Biomimetic Catalysis System Coupling Polyoxometalates with Deep Eutectic Solvents for Selective Aerobic Oxidation Desulfurization. *Appl. Catal. B Environ.* 2019, 259, 118089.
- (18) Mukhacheva, A. A.; Volchek, V. V.; Yanshole, V. V.; Kompankov, N. B.; Gushchin, A. L.; Benassi, E.; Abramov, P. A.; Sokolov, M. N. Is It Possible To Prepare a Heterometal Anderson–Evans Type Anion? *Inorg. Chem.* 2020, 59 (4), 2116–2120. <https://doi.org/10.1021/acs.inorgchem.9b02898>.
- (19) Hasenknopf, B.; Micoine, K.; Lacôte, E.; Thorimbert, S.; Malacria, M.; Thouvenot, R. Chirality in Polyoxometalate Chemistry. *Eur. J. Inorg. Chem.* 2008, 2008 (32), 5001–5013. <https://doi.org/10.1002/ejic.200800759>.
- (20) Cronin, L. Supramolecular Coordination Chemistry. *Annu. Rep. Sect. AInorganic Chem.* 2006, 102, 353–378.
- (21) Judd, D. A.; Nettles, J. H.; Nevins, N.; Snyder, J. P.; Liotta, D. C.; Tang, J.; Ermolieff, J.; Schinazi, R. F.; Hill, C. L. Polyoxometalate HIV-1 Protease Inhibitors. A New Mode of Protease Inhibition. *J. Am. Chem. Soc.* 2001, 123 (5), 886–897. <https://doi.org/10.1021/ja001809e>.
- (22) Vasylyev, M. V.; Neumann, R. New Heterogeneous Polyoxometalate Based Mesoporous Catalysts for Hydrogen Peroxide Mediated Oxidation Reactions. *J. Am. Chem. Soc.* 2004, 126 (3), 884–890. <https://doi.org/10.1021/ja036702g>.
- (23) G.M. Sheldrick, SHELXL-2013, University of Göttingen, Germany, 2013.
- (24) A.L. Spek, PLATON, Utrecht University, The Netherlands, 2001.
- (25) FT-IR Spectroscopy-Attenuated Total Reflectance (ATR), Perkin Elmer Life and Analytical Sciences (2005).
- (26) An, H.; Wang, E.; Xiao, D.; Li, Y.; Xu, L. Self-Assembly of a Novel 3D Open Framework from Anderson-Type Polyoxoanions. *Inorg. Chem. Commun.* 2005, 8 (3), 267–270.
- (27) Wu, P.; Yin, P.; Zhang, J.; Hao, J.; Xiao, Z.; Wei, Y. Single-Side Organically Functionalized Anderson-Type Polyoxometalates. *Chem. – Eur. J.* 2011, 17 (43), 12002–12005. <https://doi.org/10.1002/chem.201101552>.
- (28) An, H.; Li, Y.; Wang, E.; Xiao, D.; Sun, C.; Xu, L. Self-Assembly of a Series of Extended Architectures Based on Polyoxometalate Clusters and Silver Coordination Complexes. *Inorg. Chem.* 2005, 44 (17), 6062–6070. <https://doi.org/10.1021/ic050636x>.
- (29) An, H.; Xu, T.; Wang, E.; Meng, C. A Pillar-Layered Three-Dimensional Open Framework Constructed from Polyoxometalate-Supported Metal Coordination Complex Layers and Bi-Supporting Polyoxometalate Clusters. *Inorg. Chem. Commun.* 2007, 10 (12), 1453–1456.
- (30) An, H.; Li, Y.; Xiao, D.; Wang, E.; Sun, C. Self-Assembly of Extended High-Dimensional Architectures from Anderson-Type Polyoxometalate Clusters. *Cryst. Growth Des.* 2006, 6 (5), 1107–1112. <https://doi.org/10.1021/cg050326p>.
- (31) Yaffa, L.; Kama, A. B.; Fall, B.; Traoré, B.; Diop, C. A.; Sidibé, M.; Diop, M.; Gautier, R. Synthesis, Crystal Structure and Electrochemical Properties of a New Methylammonium Sodium Decavanate Salt Na₃(CH₃NH₃)₃[V₁₀O₂₈](CH₃NH₂). 14H₂O. *J. Mol. Struct.* 2022, 1254, 132321.
- (32) Thabet, S.; Ayed, B.; Haddad, A. A Novel Organic-Inorganic Hybrid Based on Anderson-Type Polyoxometalate: H(C₅N₅H₅)₂(C₅N₅H₆)₂[Al(OH₆)Mo₆O₁₈]•10H₂O. *Bull. Mater. Sci.* 2014, 37 (6), 1503–1508. <https://doi.org/10.1007/s12034-014-0103-5>.
- (33) Dessapt, R.; Collet, M.; Coué, V.; Bujoli-Doeuff, M.; Jobic, S.; Lee, C.; Whangbo, M.-H. Kinetics of Coloration in Photochromic Organoammonium Polyoxomolybdates. *Inorg. Chem.* 2009, 48 (2), 574–580. <https://doi.org/10.1021/ic8013865>.
- (34) Wang, Y.; Zhang, L. C.; Zhu, Z. M.; Li, N.; Deng, A. F.; Zheng, S. Y. Assembly of Four Copper(II)–2,2′-Biimidazole Complex-Supported Strandberg-Type Phosphomolybdates. *Transit. Met. Chem.* 2011, 36 (3), 261–267. <https://doi.org/10.1007/s11243-011-9464-4>.

- (35) Coué, V.; Dessapt, R.; Bujoli-Doeuff, M.; Evain, M.; Jobic, S. Synthesis, Characterization, and Photochromic Properties of Hybrid Organic–Inorganic Materials Based on Molybdate, DABCO, and Piperazine. *Inorg. Chem.* 2007, 46 (7), 2824–2835. <https://doi.org/10.1021/ic0621502>.
- (36) Dessapt, R.; Gabard, M.; Bujoli-Doeuff, M.; Deniard, P.; Jobic, S. Smart Heterostructures for Tailoring the Optical Properties of Photochromic Hybrid Organic–Inorganic Polyoxometalates. *Inorg. Chem.* 2011, 50 (18), 8790–8796. <https://doi.org/10.1021/ic200653d>.
- (37) Yaffa, L.; Kama, A. B.; Sall, M. L.; Diop, C. A.; Sidibé, M.; Giorgi, M.; Diop, M.; Gautier, R. Role of the Organic Counterions on the Protonation of Strandberg-Type Phosphomolybdates. *Polyhedron* 2020, 191, 114795.
- (38) Xu, Z.; Xi, P.; Chen, F.; Zeng, Z. Synthesis and Characterization of a Novel Anderson-Type Tungstotellurate Decorated by Transition Metal Complexes: $[\text{Na}(\text{H}_2\text{O})_3]_2[\{\text{Cu}(2,2'\text{-Bipy})_2\}_2(\text{TeW}_6\text{O}_{24})] \cdot 4\text{H}_2\text{O}$. *Transit. Met. Chem.* 2008, 33 (2), 237–241. <https://doi.org/10.1007/s11243-007-9004-4>.
- (39) Dridi, H.; Boulmier, A.; Bolle, P.; Dolbecq, A.; Rebilly, J.-N.; Banse, F.; Ruhlmann, L.; Serier-Brault, H.; Dessapt, R.; Mialane, P.; Oms, O. Directing the Solid-State Photochromic and Luminescent Behaviors of Spiromolecules with Dawson and Anderson Polyoxometalate Units. *J. Mater. Chem. C* 2020, 8 (2), 637–649. <https://doi.org/10.1039/C9TC05906G>.